(NASA-CR-123770) DYNAMIC HOLOGRAPHIC STORAGE IN LITHIUM NIOBATE Final Report
H. Aronson (Isomet Corp., Oakland, N.J.)
May 1972 45 p CSCL 20E G3/16

N72-30444
Unclas
15902

ISOMET

Final Report on

Contract No. NAS8-26635

DYNAMIC HOLOGRAPHIC STORAGE IN LITHIUM NIOBATE

CR-123770

DRA

May, 1972

Harmon Aronson

Sponsored by:

National Aeronautics and Space Administration
Marshall Space Flight Center
Huntsville, Alabama

Isomet Corporation
103 Bauer Drive
Oakland, New Jersey 07436

ISOMET

TABLE OF CONTENTS

ISOMET

TABLE OF CONTENTS
(continued)

ISOMET

LIST OF TABLES

ISOMET

LIST OF FIGURES AND PHOTOGRAPHS

ISOMET

ABSTRACT

A program was undertaken to improve the optical recording properties of $LiNbO_3$ for holographic optical memory application. Iron, copper, and manganese doping were all found to increase the optical sensitivity of $LiNbO_3$. Over two orders of magnitude improvement was obtained, resulting in an exposure of 366 $\mu J/mm^2$ to obtain 1% efficiency in $LiNbO_3$:Fe. High quality pictorial information was stored in 1mm diameter holograms.

1.0 INTRODUCTION

The principal aim of this investigation was to improve the holographic recording and storage properties of single crystal lithium niobate ($LiNbO_3$) for optical memory application.

During the course of this study it was found that doping $LiNbO_3$ with iron, copper, or manganese resulted in substantial improvement in the recording properties of the crystal. The most spectacular results were obtained with iron doping, where an improvement in optical sensitivity of over two orders of magnitude were measured. In addition, there is evidence that the doped crystals have increased thermal lifetimes. Thus, the two major objections that were raised against the use of $LiNbO_3$ for optical memory planes, the low optical sensitivity and limited thermal lifetime, have been overcome by doping the crystal and doped $LiNbO_3$ is, in our opinion, the most promising material for dynamic optical recording.

This work was begun because of the realization that all of the erasable recording materials which were being considered for this application had inherent limitations which offered little hope for solution. These were the photochromics, ferromagnetic thin films, and thermoplastics. The first two classes of materials store holograms which yield low diffraction efficiency upon reconstruction. Ferromagnetic films in addition, require large optical energy for writing. The difficulties with thermoplastics are the complicated arrangements needed for writing and the eventual fatigue of the material after multiple write-read-erase cycles due to polymer cross linking.

The class of ferroelectric crystals (such as $LiNbO_3$), on the other hand, store phase, volume holograms which result in high diffraction efficiency and added storage capacity because of the use of the thickness dimension. Furthermore, the writing mechanism involves the motion of photoexcited electrons, a process which is both reversible and non-destructive.

The drawbacks of the ferroelectric crystals did not appear to be inherent in the material or recording process, and means were proposed to overcome these limitations. After a years effort, research at Isomet and other laboratories affirmed the early enthusiasm on $LiNbO_3$ for optical recording applications as suitable doping was found to substantially increase the sensitivity and lengthen the storage lifetime.

During the course of the contract, pure $LiNbO_3$ and Fe, Cu, and Mn doped crystals were delivered to Marshall Space Flight Center.

2.0 IMAGING PROPERTIES OF PHASE, VOLUME HOLOGRAMS

2.1 Volume Holograms

As a prelude to a discussion of our experimental results on storing phase holograms in doped $LiNbO_3$, we will review the theory of the imaging properties of such holograms. The results presented in this section are true for any material which supports a phase, volume hologram, and not limited to $LiNbO_3$

Holography is an imaging process in which both the amplitude and phase of light diffracted by an object is recorded in a photosensitive medium. The more familiar photographic recording stores only intensity information.

Since all photosensitive materials respond to optical energy (intensity), the added phase information is obtained by forming the interference pattern of the light diffracted by an object with a light of known phase. In that region of space where the two waves overlap, by the superposition principle of optics the optical wave is the sum of the object and reference wave amplitudes. Using the complex representation, the total optical amplitude at each instant of time is

$$(1) \qquad \vec{A}(x,t) = \vec{a}_o(x)\, e^{i\phi_o(x,t)} + \vec{a}_r(x)\, e^{i\phi_r(x,t)} \quad ,$$

where $\vec{a}$ and ϕ are the amplitude and phase of the waves, which in general depend on poxition x. For plane waves $\vec{a}(x)$ = constant, $\phi(\vec{x}) = \vec{k}\cdot x$. For spherical waves $\vec{a}(\vec{x}) = \frac{\vec{a}}{r}$, $\phi = kr$, $r = |\vec{x}|$.

The intensity contains an interference term which gives the phase information.

$$(2) \qquad I(x,t) \equiv |A|^2 = a_o^2 + a_r^2 + 2\vec{a}_o \cdot \vec{a}_r \cos(\phi_o - \phi_r).$$

Our first observation from eq.(2) is that the polarization of the two beam waves must be essentially parallel for interference to occur.

Since all recording processes take a finite amount of time, the time average of the instantaneous intensity is required.

For monochromatic waves $\phi(x,t) = \phi(x) - iwt$, with $w = 2\pi f$, the circular frequency.

(3) Set $\phi_o(\vec{x}) - \phi_r(\vec{x}) = \Delta\phi$, $w_o - w_r = \Delta w$

$$I(\vec{x}) = \frac{1}{T}\int_o^T I(x,t)\,dt$$

Then from (2) one obtains

$$(4) \qquad I(\vec{x}) = a_o^2 + a_r^2 + \frac{2\vec{a}_o}{T} \cdot \vec{a}_r \int_o^T \cos(\Delta\phi - \Delta wt)\,dt$$

From the identity $\cos(a-b) = \cos a \cos b + \sin a \sin b$ (4) can be written in a form easily integrated

$$I(\vec{x}) = a_o^2 + a_r^2 + \frac{2a_o \vec{\cdot}\, a_r}{T} \int_0^T (\cos \Delta\phi \cos \Delta wT + \sin \Delta\phi \sin \Delta wT)\,dt \qquad (5)$$

Inspection of eq.(5) shows that the integral of the sinusoidal terms gives zero unless $\Delta wT \ll 1$.

Mathematically,

$$I(\vec{x}) = a_o^2 + a_r^2 \qquad (\Delta wT > 1) \qquad (6a)$$

$$I(\vec{x}) = a_o^2 + a_r^2 + 2a_o \vec{\cdot}\, a_r \cos \Delta\phi \qquad (\Delta wT < 1) \qquad (6b)$$

For laser recording, $\Delta wT < 1$ and the interference term is recorded. Eq.(6a) shows that if the frequency of one of the two beams is shifted, the other must also in order to record the interference pattern. This must be kept in mind when using acousto-optic devices, which frequency shift the light by an amount equal to the acoustic frequency, typically 100-300 MHz.

From eq.(6b) we see that the interference pattern is a three dimensional function. If a photosensitive medium is placed in the region of space where the two interfere, this three dimensional pattern will be recorded throughout the volume of the medium. This is referred to as a volume hologram. A plane hologram is formed when

C

a photosensitive medium records only a planar slice of the interference pattern.

The fringe pattern which is recorded throughout the depth of a volume hologram acts as a three dimensional optical diffraction grating. Reconstruction of the image occurs upon illumination of the hologram, whereupon, the light diffracted from the grating will form a real or virtual image of the object.

An analysis [1] shows that a real image will be obtained when the illuminating beam is the conjugate to the reference beam, while a virtual image is formed when the illuminating beam coincides with the reference beam. This is illustrated in Figure 1.

2.2 Recording Volume Hologram

We will list, without proof, some of the equations relevant for phase, volume holograms. These equations may be derived by solving the coupled differential equations which describe the diffraction of light from a volume diffraction grating [2]. More simply, if one makes use of the analogy of volume holography to Bragg diffraction in acousto-optics, one may transcribe many of the acousto-optic equations already derived [3].

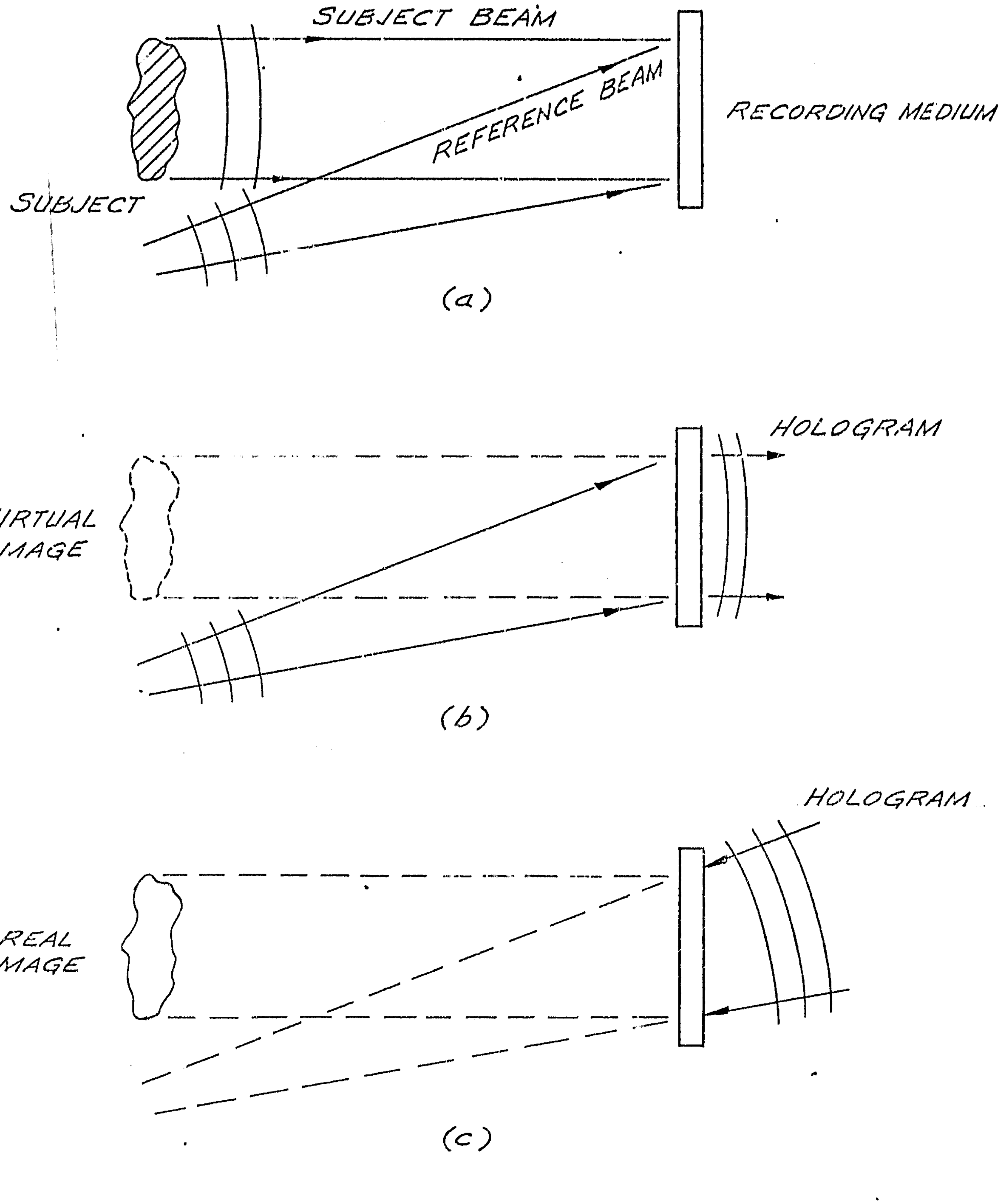

FIGURE (1) - Holographic Formation and Reconstruction
(a) formation of hologram
(b) reconstruction of virtual image, using the original reference beam to illuminate the hologram
(c) reconstruction of real image, using the conjugate to the reference beam

We consider the simplest case of the hologram formed by the interference of two plane waves as shown in Figure 2. The intensity of the interference pattern is easily derived and is given by

(7) $$I = 2I_o(1 + \cos \frac{2\pi Z}{d}),$$

(8) with $$1/d = \frac{2\sin\phi}{\lambda_w} .$$

I_o is the intensity of each wave, $2I_o$ the total intensity of both waves without interference, and the cosine term describes the interference.

The spatial frequency of the interference pattern is given by d^{-1}, and can be varied by changing the angle, 2ϕ, between the two waves. We will distinguish between the wavelengths used for writing and reading by the subscripts W and R.

For the recording and reconstruction of a more general intensity pattern, the following analysis will hold for each Fourier component and the resultant may be obtained by summation for linear media. Note that eq.(8) gives the same result inside or outside the medium by virtue of Snell's law.

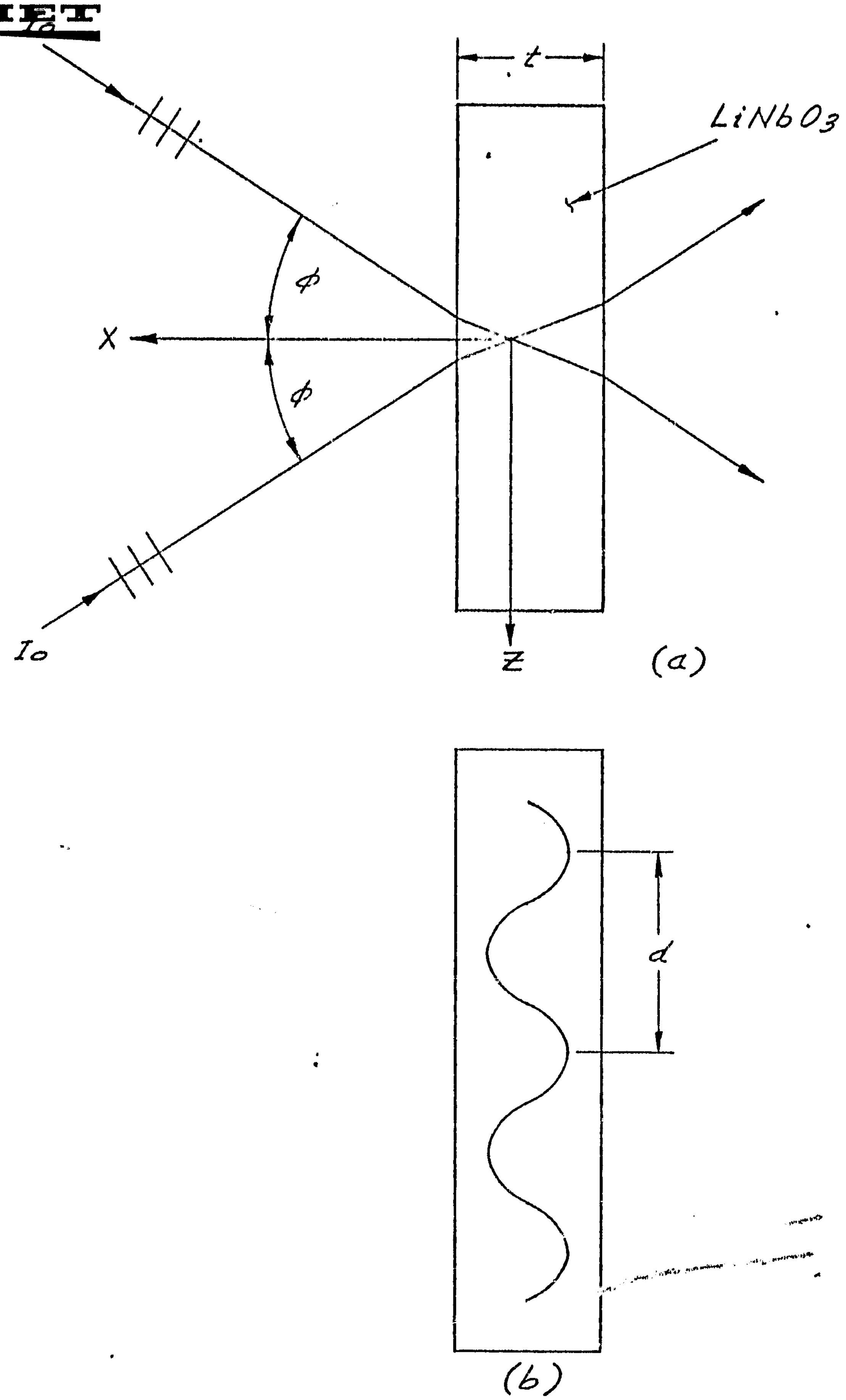

FIGURE (2) - Holographic Recording of Two Beam Interference Pattern (a) Geometry of the recording process. (b) Sinusoidal interference pattern which is recorded in the $LiNbO_3$. The spatial frequency is d^{-1}.

2.3 Minimum Thickness of a Volume Hologram

The thickness of the hologram must be greater than some minimum value for it to exhibit the properties of a volume hologram-angular selectivity and a single diffracted order upon reconstruction.

The minimum thickness is given by

$$t_{min} = \frac{.955\ n\ d^2}{\lambda_r} \tag{9}$$

λ_r is the wavelength used for reading as measured in air, and n, the average index of refraction, converts λ_r to its value inside the recording medium. The value of d is given by equation (8).

Typically, t must be large compared to λ. To see this, set $\lambda_w = \lambda_r = \lambda, \phi = 30^\circ$. Using eqs.(8), (9) we obtain

$$t_{min} \simeq n\lambda \simeq 10^{-3}\ \text{mm}$$

when $n \simeq 2$ ($LiNbO_3$ $n = 2.3$)

The minimum thickness of the $LiNbO_3$ crystal used in any experiment was 1mm, a value much greater than the minimum needed for a volume hologram.

2.4 Reconstruction Efficiency

The stored image is reconstructed by illuminating the hologram with the reference beam only. Part of the beam gets diffracted from the volume, phase grating which is formed by the hologram.

For the case of no optical absorption, the fraction of the incident optical intensity which appears in the image is given by

$$\frac{I_1}{I_o} = \sin^2 \frac{\pi \Delta n t}{\lambda_r \cos\theta} \qquad (10)$$

where Δn is the peak value of the assumed sinusoidal variation in index of refraction, t the thickness of the hologram, λ_r the wavelength used for reading, and θ the angle of incidence as measured in the medium. When this fraction is expressed as a percent, it is called either the recontruction efficiency or the diffraction efficiency and denoted by η.

2.5 Bragg Angle and Angular Bandwidth

As is well known, volume holograms exhibit angular selectivity, which allows for multiple storage at the same location by storing holograms at different angular positions. To read out any particular hologram, the reading beam must be incident at the correct angle corresponding to the hologram being interrogated.

For the sinusoidal grating, the angle of incidence must equal θ_b, which is given by the equation

$$\sin\theta_b = \frac{\lambda_r}{2d} = \frac{\lambda_r}{\lambda_w}\sin\phi \tag{11}$$

where the second equality was obtained using eq.(8). θ_b is also referred to as the Bragg angle. When the same wavelength is used for reading as was used for writing, the readout beam must be aligned along the reference beam ($\theta_b = \phi$). When $\lambda_r \neq \lambda_w$, the angle of incidence must differ from the angle of the reference beam according to equation (11).

When the incident angle differs from the Bragg angle the reconstruction efficiency is reduced from that given by (10). As the deviation from Bragg incidence is further increased, the efficiency will finally drop to zero. The angular excursion which results in the efficiency to drop by 50% is generally taken to be the angular bandwidth.

This half power angular bandwidth as measured in air is given by the equation

$$\Delta\theta = \frac{.9nd}{t} \tag{12}$$

These equations give us the theoretical framework in which to analyze many of our experimental results on storing volume holograms in $LiNbO_3$.

3.0 PHYSICAL MECHANISM OF OPTICAL RECORDING IN $LiNbO_3$

Optical recording in $LiNbO_3$ is a purely physical process which depends on photoexcitation of electrons and the electro-optic effect. The basic phenomena that is observed is that the crystal exhibits small changes in the index of refraction after exposure to intense light. There is no accepted name for this photo-induced refractive index change.

One model [4] for this phenomena assumes that when light is incident on $LiNbO_3$, electrons are photoexcited in those regions of the crystal of high optical intensity. The photoexcited electrons migrate in the crystal, becoming trapped and optically re-excited until they are trapped in regions of the crystal where the optical intensity is low. The net result is a buildup of negative charge in dark regions due to the accumulation of electrons, and positive charge in the areas of the crystal which were under illumination due to the loss of electrons. The charges will continue to build up until an equilibrium distribution is reached. At each instant of time during the process an electric field is generated by the charge distribution. The model then assumes that this electric field modulates the index of refraction through the electro-optic effect. The maximum value obtained by Δn occurs when the charge distribution reaches equilibrium.

From eq.(10) we find that for crystals 1mm thick, 100% diffraction efficiency will be obtained when Δn is of the order 10-4.

The addition of the dopants iron, copper, and manganese have been found to greatly increase the sensitivity of $LiNbO_3$ for recording. While the role played by these dopants is not fully understood at this time, they probably affect any one of the following properties, each of which will increase the sensitivity:

(a) increase the concentration of trapping centers
(b) increase the number of free carries
(c) increase the optical absorption cross section

Some unresolved questions concern the migration mechanism (drift vs diffusion of electrons through the lattice) [5] and the origin of the field which produces the electro-optic effect [6].

4.0 CRYSTAL GROWTH, FABRICATION, AND PROPFRTIES

4.1 Growth and Fabrication

Lithium niobate is grown from the melt by the Czochralski method [7]. Photograph 1 shows a Czrochralski crystal puller and controller. The dopants were added to the melt in concentrations ranging from 0.01 to 0.5 weight percent. After growth, slices of each crystal were chemically analyzed to determine the exact concentration of dopant which resulted. The dopants and concentration of all of the crystals grown during the course of this contract are given in Table I. The crystals were of good optical quality, with large areas of the crystal free from cracks, flaws and imperfections. The boules were typically 1-1/2 inches long along the C-axis and 1/2 inch in diameter. This size was chosen for convenience, and does not represent the size boules of $LiNbO_3$ can be grown. Undoped $LiNbO_3$ has already been grown at Isomet in lengths exceeding 5 inches along the C-axis and diameter exceeding 1 inch.

The color of pure lithium niobate crystal is water white. The addition of small quantities of dopant drastically changed the color, from blue due to cobalt doping to deep red resulting from iron doping. The dopants which resulted in an increased sensitivity in optical recording all gave the crystal a reddish color, which indicates that absorption in the blue part of the spectrum was increased. However, if a particular dopant produced a reddish tint in the crystal, this was not always a guarantee that the sensitivity would be increased.

X

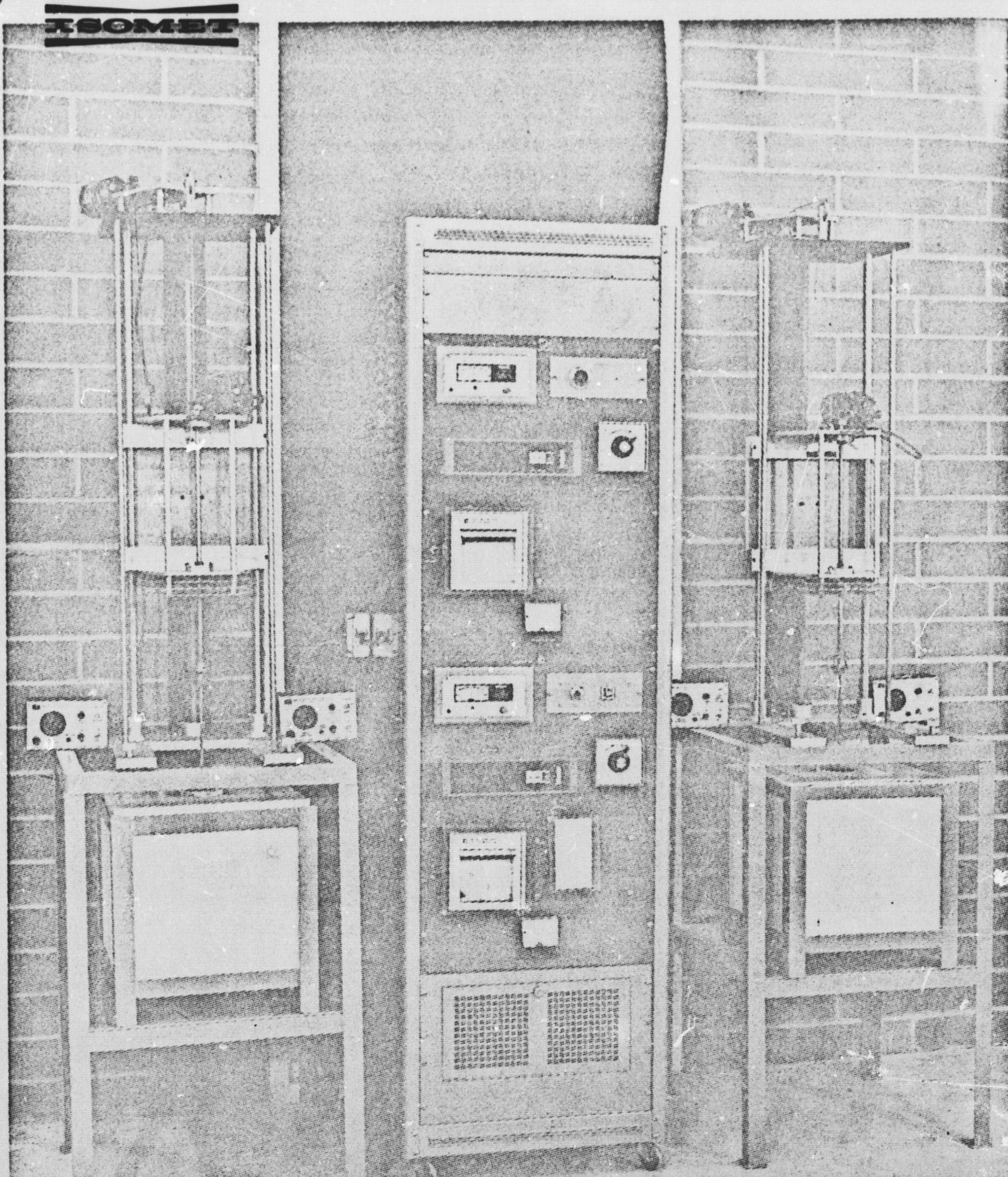

PHOTOGRAPH 1 - CZOCHRALSKI CRYSTAL PULLER

The crystals were grown in resistance heated furnaces. The starting material was chemically analyzed using a mass spectrograph.

The major impurities in the starting material, expressed as ppm, wt., are

Ta	50 ppm
K, Ca, Fe	each 20 ppm
F, Na, Mg, Al, S	each 10 ppm

The concentration of all other elements is less than 10 ppm.

The starting $LiNbO_3$ was the stoichiometric composition.

The pure $LiNbO_3$ and the dopant to be used were weighed separately, mixed, and then melted in a pure platinum crucible. For iron doping, for example, 303.99 grams of $LiNbO_3$ were mixed with 0.329 grams of Fe_2O_3. A seed crystal (C-axis) was introduced into the melt after the growth chamber reached thermal equilibrium. The crystal was then grown in an air atmosphere using a pulling rate of 0.132 inches/hr and a rotation rate of 28 rpm. After growth was completed, the crystal was cooled over a seventeen hour period to room temperature. The boule was then oxygen annealed for twenty hours at 1000°C using heating and cooling rates of 50°C/hr. The crystal was X-ray orientated to locate the a and c axes.

Parallel flats were then placed on the boule perpendicular to the C-axis and platinum electrodes applied. The boule was then poled by standard techniques and re-annealed at 900°C.

The crystal was then sliced 1mm thick along the A-axis. The A-faces were polished parallel to 1 arc second and flat to $\lambda/2$. The polished crystal was mounted on a metal stand for ease in optical testing.

TABLE I

Doped $LiNbO_3$ Crystals Grown During Course of Contract

Isomet No.	Dopant	Conc. in Melt Weight Percent	Conc. in Crystal Weight Percent	
			(Nb_2O_5)	(Li_2O)
100	pure	--	50.25Mole %	49.75Mole %
101	Nb	3	50.3	49.7
102	Nb	5	51.18	48.82
103	Nb	10	51.85	48.15
104	Nb	20	51.39	48.61
105	V	0.1	*	
106-108	V	0.5	*	
109	Fe	0.055	*	
110	Fe	0.0275	*	
111	Cr	0.01	*	
112	--	--	-	
113	Cr	0.05	0.05	
114	Cu	0.1	0.01	
115	Cu	0.2	0.04	
116	Cu	0.05	0.009	
117	Mn	0.05	0.03	
118	Mn	0.1	0.05	
119	Mn	0.5	0.22	
120	Ni	0.05	0.02	
121	Ni	0.1	0.05	
122	Ni	0.5	0.18	
123	Ti	0.05	*	

TABLE I
(continued)

124	Ti	0.1	*
125	Co	0.05	0.02
126	Co	0.1	0.03
127	Fe	0.1	0.07
128	--	--	-
129	Er	0.05	*
130	Er	0.1	*
131	U	0.05	*
132	U	0.1	*
133	Fe	0.1	*
134	Fe	0.2	*
135	Cu	0.2	*

*Concentration of dopant in crystal not determined for these crystals.

4.2 Optical Transmission

The optical transmission of each type of crystal grown was measured using a Cary 14 Spectro-photometer. The transmission curves versus optical wavelength for some of the more important dopants are given in Figures 3 and 4. The transmission extends from .4μ to 5μ for undoped $LiNbO_3$ crystals.

The transmission is reduced from 100% by optical reflections at each surface and absorption through the thickness, t, of the crystal. This is expressed mathematically by the equation

$$T = \frac{(1-R)^2 e^{-at}}{1-R^2 e^{-2at}} \qquad (13)$$

where R is the intensity reflection factor which is given by the Fresnel formulas. For normal incidence, this is simply

$$R = \left(\frac{n-1}{n+1}\right)^2 . \qquad (14)$$

The absorption coefficient is denoted by 'a' and the thickness by t. The second term in the denominator of equation (13) represents multiple reflections in the crystal.

Both the absorption coefficient and the reflection factor depend on wavelength and optical polarization.

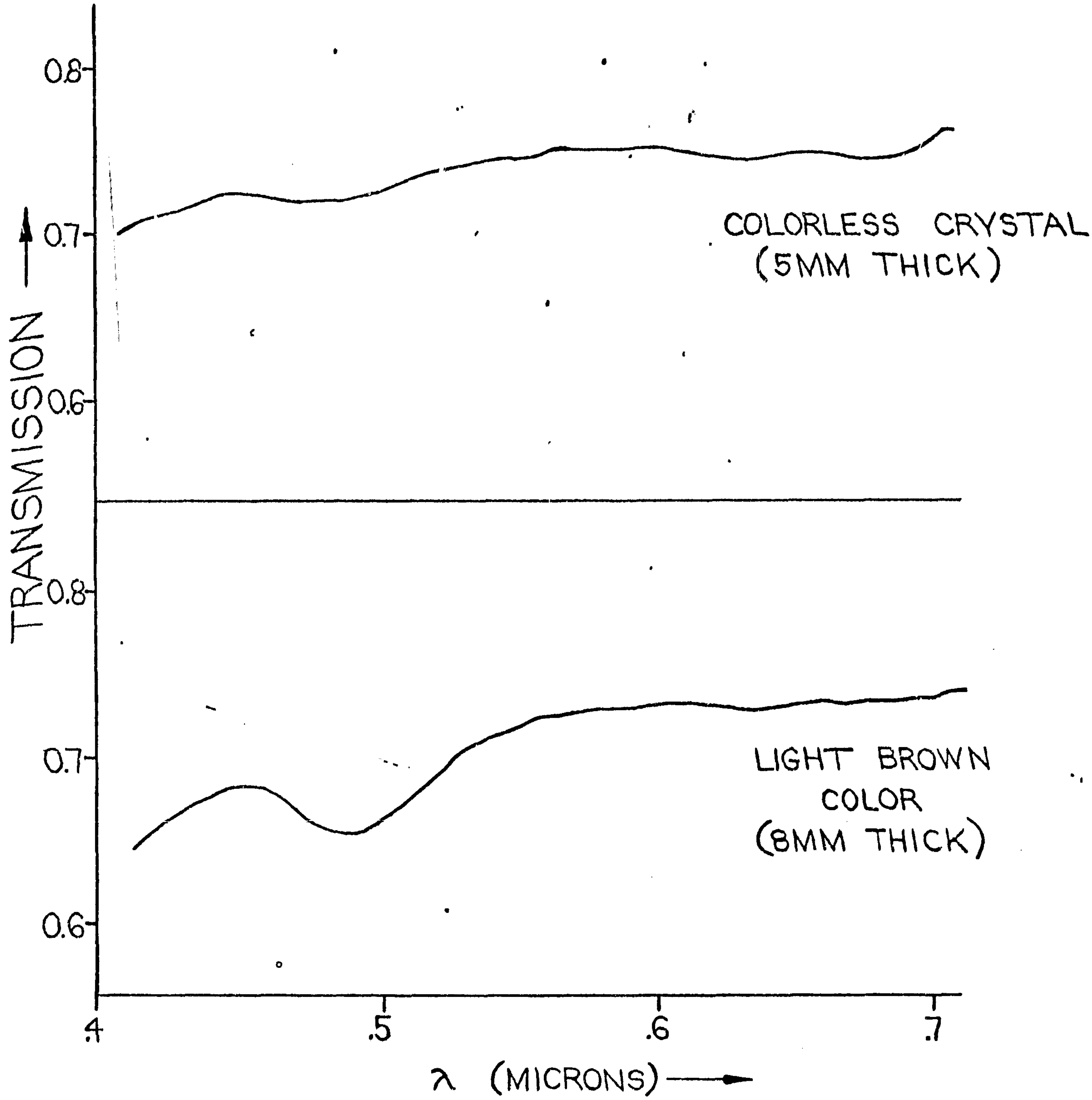

FIGURE - 3
OPTICAL TRANSMISSION FOR UNDOPED
$LiNbO_3$

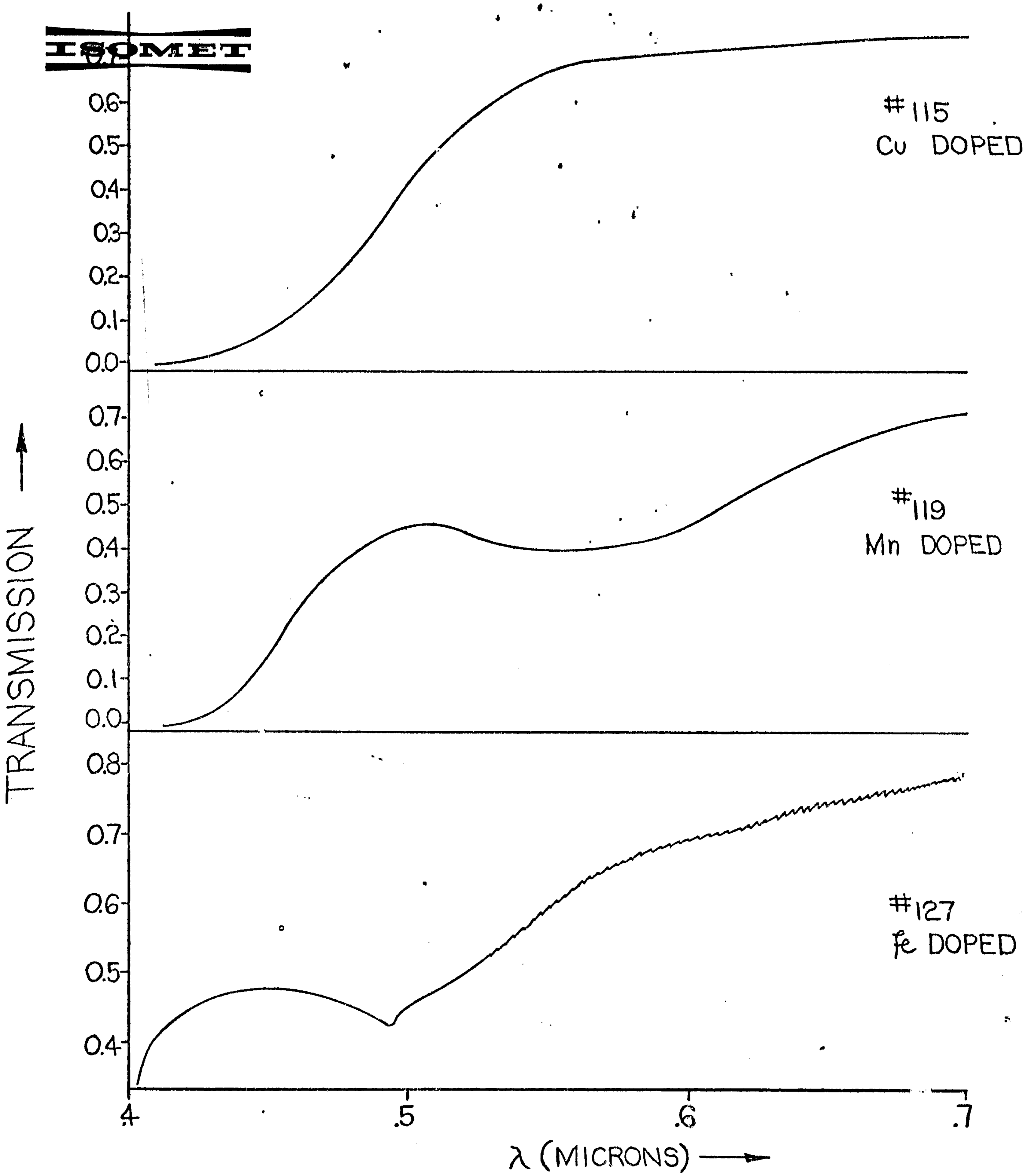

FIGURE-4

Optical transmission for some doped $LiNbO_3$ crystals. These dopants greatly increased the recording sensitivity of $LiNbO_3$. Thickness of each crystal = 1mm.

The transmission measurements, however, were made with unpolarized light, so that separate values of the absorption coefficient for ordinary and extraordinary polarized cannot be determined.

From eq.(14) and the index of refraction for $LiNbO_3$ ($n \sim 2.3$) we find that the loss due to reflections is approximately 15.5% per surface which results in a transmission for light passing through 2 surfaces of 71.5%. By coating the optical faces with a suitable dielectric coating (AR coating) the reflection losses can be kept to under 1%.

4.3 Index of Refraction

The index of refraction of pure $LiNbO_3$ is given in Table II after Boyd et. al. [8].

TABLE II

Index of Refraction of Undoped $LiNbO_3$

$\lambda (\mu)$	n^o	n^e
0.42	2.4089	2.3025
0.45	2.3780	2.2772
0.50	2.3410	2.2457
0.55	2.3132	2.2237
0.60	2.2967	2.2082
0.70	2.2716	2.1874
0.80	2.2571	2.1745
0.90	2.2448	2.1641
1.00	2.2370	2.1567
1.20	2.2269	2.1478
1.40	2.2184	2.1417
1.60	2.2113	2.1361
1.80	2.2049	2.1306
2.00	2.1974	2.1250
2.20	2.1909	2.1183
2.40	2.1850	2.1129
2.60	2.1778	2.1071
2.80	2.1703	2.1009
3.00	2.1625	2.0945
3.20	2.1543	2.0871
3.40	2.1456	2.0804
3.60	2.1363	2.0725
3.80	2.1263	2.0642
4.00	2.1155	2.0553

4.4 Addition Physical Properties of $LiNbO_3$

$LiNbO_3$ is a uniaxial crystal with point group symmetry (3m). The crystal has piezoelectric, ferroelectric, and electro-optic properties. Its' Curie temperature is $1160^{\circ}C$, the highest of the known ferroelectrics. The density is 4.7 gm/cm^3.

For crystals in class 3m there are six independent elastic, four independent piezoelectric, and two independent dielectric constants. The dielectric constants are $\varepsilon^{s}_{11}/\varepsilon_o = 44$ and $\varepsilon^{s}_{33}/\varepsilon_o = 29$.

The thermal expansion coefficients are $\alpha_a = 16.7ppm/^{\circ}C$ and $\alpha_c = 2.0ppm/^{\circ}C$ over the temperature range from 20 to $200^{\circ}C$.

$LiNbO_3$ has a hardness of 4.5 on the Mho scale. The optical surfaces may be easily cleaned using lens cleaner and a piece of lens paper.

5.0 RESULTS ON HOLOGRAPHIC RECORDING IN DOPED $LiNbO_3$ CRYSTALS

5.1 General Remarks on the Results

Simple two beam interference patterns were holographically recorded using the test setup shown in Figure 5. The crystallographic C-axis of the $LiNbO_3$ must bear a particular orientation to the optical beams during both recording and reconstruction. During recording, the C-axis must lie in the plane formed by the reference and object beams and be oriented approximately perpendicular to the bisector of the two beams. The recording process is independent of the polarization of the light, as long as the polarization of both beams are approximately parallel. During reconstruction the reference beam or its conjugate illuminates the hologram. For maximum diffraction efficiency, the wave must be extraordinarily polarized (polarization parallel to the C-axis). The half-wave plate shown in Figure 5 converts the vertically polarized light to horizontal polarization, so that the same setup could be used for recording and reconstruction.

The angle between the object and reference beams was approximately 12 degrees for all test except one, where it was increased to 90 degrees. By blocking off one of the beams, the formed hologram can be interrogated with the other beam.

The ratio of the light intensity which is diffracted by the hologram to the light which is transmitted through the crystal we call the diffraction efficiency. When

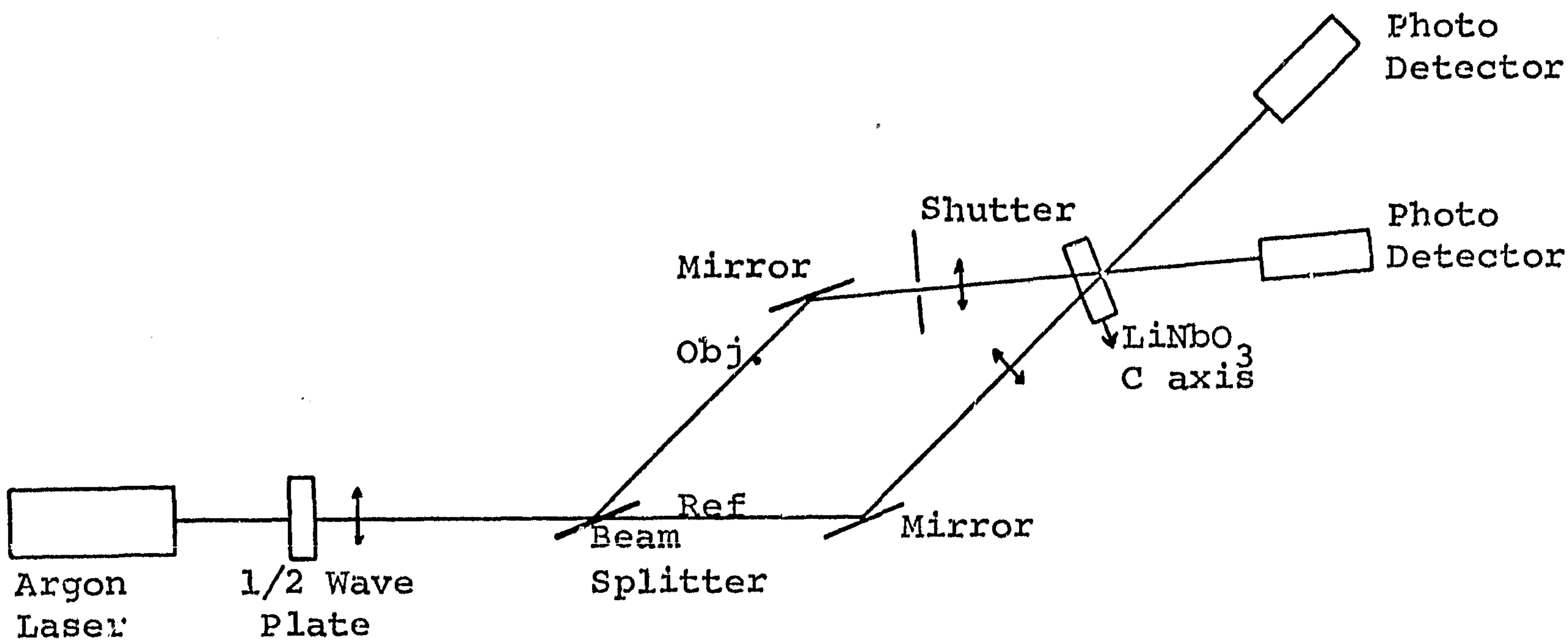

EXPERIMENTAL SETUP FOR HOLOGRAPHIC RECORDING AND READ OUT

FIGURE 5

absorption and reflection losses are taken into account, the overall efficiency of the hologram is reduced. By AR coating the optical faces of the crystal, the reflection losses can be reduced to a few percent. If, further, the hologram is read out with a wavelength for which the absorption is low, the overall efficiency of the hologram will be high.

During the course of our experiments we have recorded high efficiency (50%) holograms requiring exposure times of seconds and investigated higher speed holography using exposure times in the range of 10 milliseconds. Because the laser power was approximately the same in both cases, the exposure available for recording in the latter case was low and the diffraction efficiency was correspondingly low (several percent).

Other experiments which were performed showed that there was no failure in reciprocity over the dynamic range in which we were working. The same set of experiments showed that for low values of diffraction efficiency, the efficiency was a linear function of exposure (exposure E=It, I the optical intensity and t the exposure time).

One unexpected result was the increase in diffraction efficiency during readout. This self-enhancement effect was observed to increase the diffraction efficiency by a factor of 2 to 5 times when the initial efficiency was a few percent. The greatest self-enhancement was observed to increase the diffraction efficiency 30-fold. The reading times were several times as long as the writing times for enhancement.

It is believed that the enhancement is due to the recording of the interference pattern formed by the diffracted wave and the reference wave. Of course, for this to enhance the diffraction efficiency, the new hologram which is formed during readout must be in phase with the hologram originally recorded.

5.2 Reconstruction Efficiency

The sensitivity of $LiNbO_3$ was found to depend strongly on the wavelength used for recording, being very sensitive in the blue and less sensitive as the wavelength is increased. This wavelength dependence can be seen from the data given in Table III, which shows the exposure required to achieve high reconstruction efficiency in an 8mm thick slice of undoped $LiNbO_3$ using the different wavelengths of an argon ion laser. The efficiency includes an increase of about 20% due to self-enhancement.

TABLE III

Reconstruction Efficiency for 8mm Thick Undoped $LiNbO_3$

λ (μm)	Exposure (J/mm^2)	η, Efficiency (%)
.5145	4.75	50
.4880	3.28	40
.4765	1.4	50

During recording, the ratio of optical power in the reference to object beams was approximately 3:1.

A comparison of the sensitivities of the crystals doped with Cu, Mn, and Fe against undoped $LiNbO_3$ is given in Table IV. The exposure was constant and equal to 770 mJ/mm^2 with an exposure time of 15 seconds. The 4880Å wavelength was used, and the ratio of the optical power in the reference to object beam was 2.3:1. The beam diameter was about 2.5mm at the crystal location.

TABLE IV

Reconstruction Efficiency for Various Doped Crystals for Constant Exposure

Isomet No. and Dopant	Crystal Thickness (mm)	Po (mW)	P_1 (mW)	$\eta = \frac{P_1}{(P_o+P_1)} \times 100$ (%)
#100, pure	5	112	.36	0.32
#119, Mn	1	21.6	1.8	7.7
#11[illegible], Cu	1	27	14.4	34.8
#127, Fe	1	16.2	16.2	50

Po denotes the optical power transmitted and P_1 the optical power in the reconstructed beam. The improvement which can be obtained by doping the crystal is apparent from Table IV.

If data on the pure $LiNbO_3$ is normalized to the thickness of the doped crystals listed in Table IV, then the efficiency would be reduced by a factor of 25, since $\eta \sim t^2$ for small (see eq.10).

Our tests on crystal #127 using small exposure times showed the crystal to have a sensitivity considerable greater than what would be inferred from Table IV. In these high speed tests, the relatively low laser power resulted in low exposures which produced low efficiency holograms. As before, efficiency is measured relative to the transmitted beam and so neglects reflection and absorption losses. The results of this test is given in Table V.

TABLE V

Reconstruction Efficiency for $LiNbO_3$:Fe

Exposure Time (msec)	Optical Intensity (mW/mm^2)	Exposure, E ($\mu J/mm^2$)	Diffraction Efficiency. After - Exposure (%)	Enhancement (%)
120	2.93	352	0.96	6.4
64	5.5	352	0.96	4.9
64	11.7	750	2.05	10.0
20	23.8	475	1.3	5.2
7	23.8	167	0.45	1.8

Several conclusions can be drawn from this data. The first is that the efficiency is a linear function of exposure, described by the equation

$$\eta = \frac{1}{366} E \quad ,$$

with η measured in percent and E in $\mu J/mm^2$. The exposure needed per 1% efficiency is then 366 $\mu J/mm^2$ per 1% efficiency. Since for small efficiency $\eta \sim (\Delta n)^2$, we can infer that $\Delta n \sim E^{1/2}$. Of course, for higher efficiencies, η will no longer remain a linear function of exposure.

The data in Table V also shows no failure in reciprocity. This opens the way for shorter exposure times by increasing the laser power.

Finally, the effect of self-enhancement, mentioned at the beginning of this chapter, can be seen from the data in the last two columns of Table V. The enhancement occurs during readout of the hologram with the reference beam only.

A wide angle hologram was stored to test the resolution of $LiNbO_3$. The angle between the reference and object beams (2ϕ) was set to 90^o, which from eq.(8) is seen to correspond to an interference pattern whose spatial frequency is 2850 lines/mm.

The ability of $LiNbO_3$ to record pictorial information was investigated by using a modification of the test setup depicted in Figure 5. A standard bar chart transparency 2 inches square was holographically stored in a 1mm diameter of a $LiNbO_3$ crystal. A beam expander was used before the transparency and a focussing lens afterward. The test setup is shown in Photograph 2, with the test pattern projected on the screen in the foreground. Figure 6

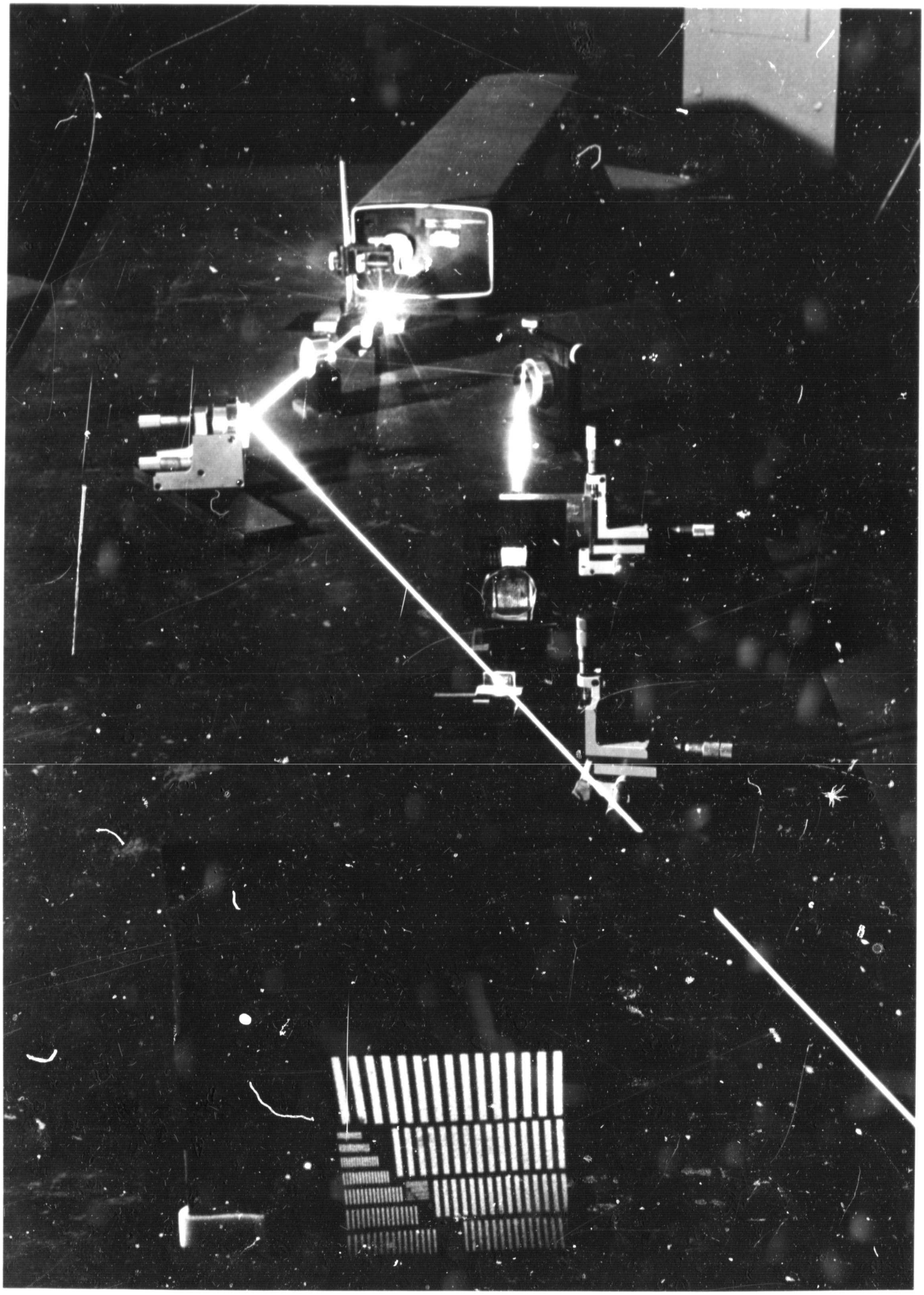

Photograph 2
Optical Setup for Storing Pictorial Information in $LiNbO_3$

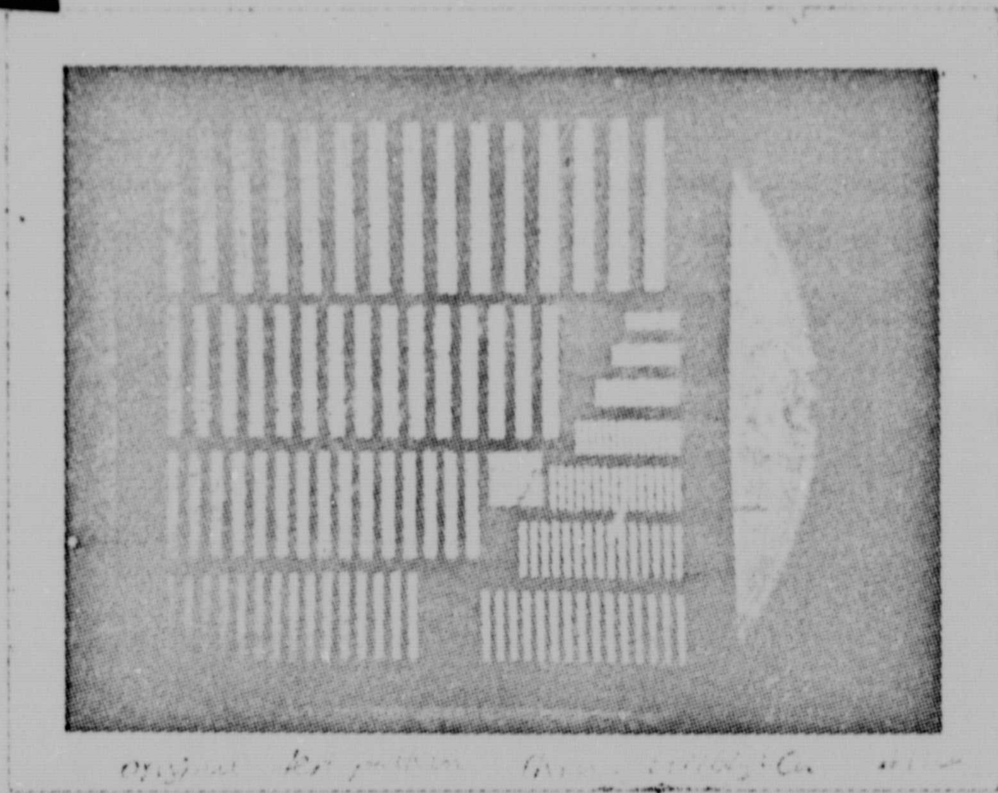

ORIGINAL TEST PATTERN THRU $LiNbO_3$:Cu No. 114

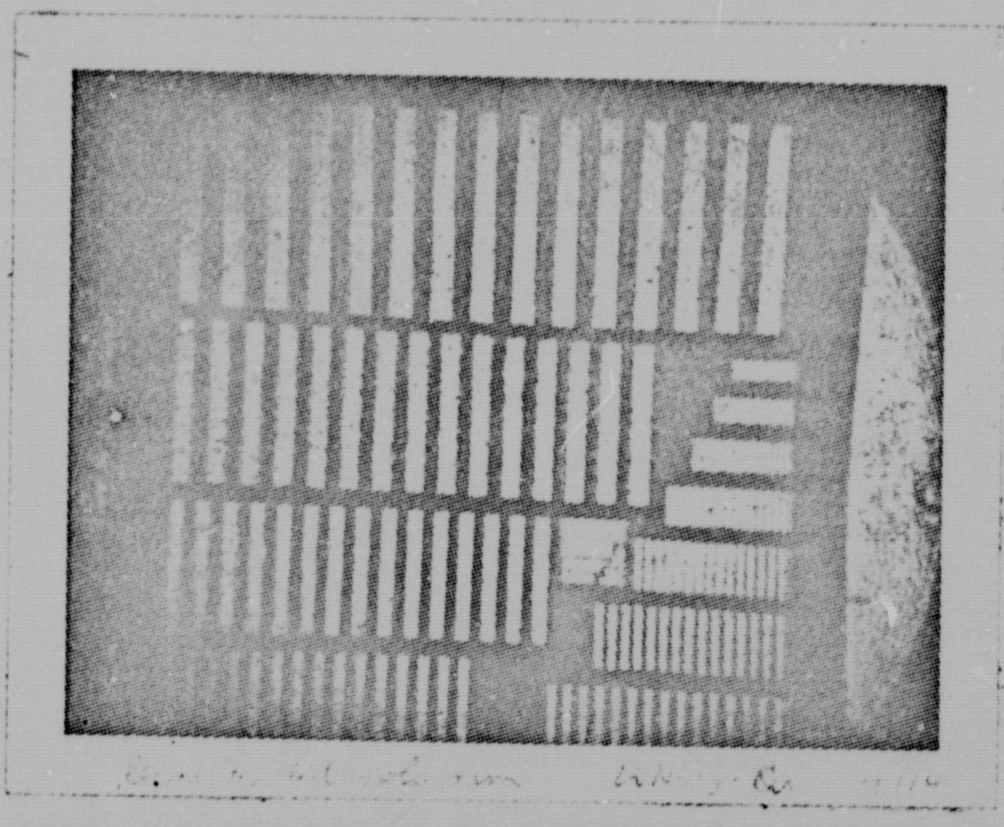

RECONSTRUCTED HOLOGRAM $LiNbO_3$:Cu No. 114

FIGURE 6

shows a photograph of the test pattern viewed through the $LiNbO_3$ and below it a photograph of the reconstruction of the test pattern which was holographically stored in the crystal. The fidelity of the recording is of high quality with good contrast ratio and reproduction of fine detail.

6.0 SUMMARY AND RECOMMENDATIONS FOR FURTHER WORK

The results of the work performed on this contract were extremely encouraging. By doping $LiNbO_3$ with iron, we were able to improve the sensitivity of the crystal over two orders of magnitude. This allowed us to store holograms with exposure times as fast as 7 milliseconds using a commercial argon laser. The resulting hologram has a diffraction efficiency of a few percent after enhancement. By increasing the exposure time, diffraction efficiencies of 50% were obtained. We also found that copper and manganese doping improved the sensitivity of $LiNbO_3$. The hologram could be readout for over 5 minutes before it began to degrade. For an average readout time of 1 millisecond, over 10^5 readouts can be performed before a refresh cycle is necessary. The recording process is reversible, and can be thermally or optically erased. The faster optical erasure is preferred.

At this point in the program we feel that doped $LiNbO_3$ holds the most promise of all the erasable recording materials for optical memory application. We feel that we have made substantial advances in improving the recording properties of $LiNbO_3$ and characterizing its performance.

Our recommendation for future works is that large array memory planes be fabricated and its performance carefully characterized. Further information is contained in our Unsolicited Technical Proposal No. 003-72, entitled "Evaluation of Large Holographic Memory Arrays of Doped Lithium Niobate".

In view of the rapid advances we made in the materials program, we feel that a continuation of a materials growth and evaluation program will be very rewarding. Further improvement in sensitivity can be expected by optimizing the concentration of dopant and investigating multiple dopings in $LiNbO_3$.

7.0 REFERENCES

[1] E.N. Leith, A. Kozma, J. Upatricks, J. Marks, and N. Massey, "Holographic Data Storage in Three Dimensional Media", Appl. Optics 5, 1303 (1966)

[2] H. Kogelnik, "Coupled Wave Theory for Thick Hologram Gratings", Bell Sept. Tech. J. 48, 2909 (1969)

[3] E.I. Gordon, "A Review of Acousto-Optical Deflection and Modulation Devices", Proc. IEEE 54, 1391 (1966)

[4] F.S. Chen, J.T. LaMacchia, and D.B. Fraser, "Holographic Storage in $LiNbO_3$", Appl. Phys. Letters 13, 223 (1968)

[5] J.J. Amodei, Appl. Phys. Letters, 18, 22 (1971)

[6] W.D. Johnston, Jr., "Optical Index Damage in $LiNbO_3$ and Other Pyroelectric Insulators", J.Appl. Phys. 41, 3279 (1970)

[7] K. Nassau, H.J. Levinstein, and G.M. Loiacono, "Lithium Niobate I and II", J. of Phys. and Chemistry of Solids, 27, 983 (1966)

[8] G.D. Boyd, R.C. Miller, K. Nassau, W.L. Bond, and A. Savage, "$LiNbO_3$: An Efficient Phase Matchable Non-linear Optical Material", Appl. Phys. Letters 5, 234 (1964)